Sea Spray Impacts on Intensifying Midlatitude Cyclones

WILL PERRIE,* EDGAR L ANDREAS,+ WEIQING ZHANG,* WEIBIAO LI,# JOHN GYAKUM,@ AND RON MCTAGGART-COWAN&

*Fisheries and Oceans Canada, Bedford Institute of Oceanography, Dartmouth, and Dalhousie University, Halifax, Nova Scotia, Canada
+U.S. Army Cold Regions Research and Engineering Laboratory, Hanover, New Hampshire
#Zhongshan University, Guangzhou, China
@McGill University, Montreal, Quebec, Canada
&The University at Albany, State University of New York, Albany, New York

(Manuscript received 29 March 2004, in final form 25 September 2004)

ABSTRACT

Air–sea transfer processes over the ocean strongly affect how hurricanes develop. High winds generate large amounts of sea spray, which can modify the transfer of momentum, heat, and moisture across the air–sea interface. However, the extent to which sea spray can modify extratropical or midlatitude hurricanes and intense cyclones has not been resolved. This paper reports simulations of extratropical Hurricanes Earl (1998) and Danielle (1998) and an intense winter cyclone from January 2000 using a mesoscale atmospheric model and a recent sea spray parameterization. These simulations show that sea spray can increase the sea surface heat flux, especially the latent heat flux, in a midlatitude cyclone and that sea spray's impact on cyclone intensity depends on the storm structure and development and is strongest for cyclones with high winds.

1. Introduction

The hurricane, one of the most energetic weather events over the ocean, is a powerful *engine* that runs on energy extracted from the ocean. The air–sea transfer of momentum and enthalpy have long been recognized as important elements for generating and maintaining hurricanes. Turbulent transfer processes over the ocean are commonly parameterized using Monin–Obukhov similarity theory. However, during high-wind, hurricane conditions, large amounts of sea spray are produced by bursting air bubbles in whitecaps and by tearing spume from the wave crests. Consequently, both turbulence and sea spray provide routes by which moisture, heat, and momentum cross the air–sea interface.

Although the question as to whether or how sea spray affects the evolution of hurricanes has been around for a long time, the answer has remained elusive. Fifty years ago, Riehl (1954) suggested that sea spray evaporation provides a significant amount of the heat needed to generate and maintain a tropical storm. In the 1970s, the sea spray problem was rediscovered (Wu 1973, 1974; Bortkovskii 1973; Ling and Kao 1976). With the Humidity Exchange Over the Sea (HEXOS) program in the mid-1980s, new ideas, better instruments, and more powerful analytical tools were brought to bear on the study of sea spray (Katsaros et al. 1987; Smith et al. 1990, 1992; Rouault et al. 1991; DeCosmo et al. 1996). However, despite the huge HEXOS effort, parameterizing sea spray and its contribution to heat fluxes remains a challenging task because the data are still quite scarce, especially for high winds.

Andreas (1992) developed a sophisticated microphysical model for the contribution of sea spray to sensible and latent heat fluxes. Fairall et al. (1994) then developed a parameterization scheme for use in numerical atmospheric models to study the effect of sea spray during hurricane development. Andreas (1998) later modified his sea spray model for application to high winds. This led to the development of the Andreas and DeCosmo (1999, 2002) spray parameterization scheme for high winds that makes it possible for us to study the impact of sea spray on hurricanes with a coupled atmosphere–ocean modeling system.

Most recent studies of sea spray focus on tropical storms because of their high wind speeds, high sea surface temperatures, and the role of sea surface fluxes. Fairall et al. (1994) claimed that, without taking account of evaporating spray droplets or some other source of latent heat, the boundary layer of modeled

Corresponding author address: Dr. William A. Perrie, Bedford Institute of Oceanography, P.O. Box 1006, 1 Challenger Drive, Dartmouth, NS B2Y 4A2, Canada.
E-mail: perriew@dfo-mpo.gc.ca

tropical cyclones would evolve in an unrealistic manner. Kepert et al. (1999) and Bao et al. (2000) investigated the impact of spray on the development of a simulated hurricane using a coupled atmosphere–ocean–wave model and found that spray increases the hurricane intensity substantially. Wang et al. (2001) reported a moderately enhanced intensity of a modeled tropical cyclone because of spray. By comparison, the effects of sea spray on extratropical storms have received less attention in the literature. Recently, Meirink and Makin (2001) used a limited-area hydrostatic model and the parameterization of Fairall et al. (1994) to study the sea spray impacts on two intense upper midlatitude (50°–70°N) storms. They suggested that the indirect effects of spray can enhance precipitation and lead to marginal intensification.

In this paper, we use a coupled atmosphere and sea spray model to simulate midlatitude Hurricanes Earl (1998) and Danielle (1998) and a severe winter storm, denoted Superbomb (2000). Our objective is to investigate the impact of sea spray on midlatitude (35°–55°N) storms over the North Atlantic. Section 2 describes the atmospheric model, the sea spray parameterization, and the experimental design of the numerical simulations. Section 3 describes the case studies; section 4 presents our results; and section 5 gives our conclusions.

2. Model description

We performed all numerical simulations with a well-tested mesoscale atmospheric model, the Canadian mesoscale compressible community model (MC2) of Benoit et al. (1997). This section describes MC2 and our bulk algorithm for turbulent air–sea fluxes, which includes a parameterization for sea spray in high winds.

a. The MC2 model

The MC2 (version 4.9.3) model has evolved as a result of cooperative research among scientists at universities and the Meteorological Service of Canada (MSC). (The model is described in more detail online at http://www.cmc.ec.gc.ca/rpn/modcom/index2.html.) MC2 originated from a limited-area model developed by Robert et al. (1985). It is a state-of-the-art, fully compressible, nonhydrostatic model that solves the full Euler equations on a limited-area Cartesian domain with time-dependent nesting of lateral boundary conditions. The planetary boundary layer is based on a prognostic equation for turbulent kinetic energy (Benoit et al. 1989, 1997) and uses the Kong and Yau (1997) microphysics package to specify prognostic equations for water vapor, cloud water, rainwater, ice particles, graupel, and to parameterize the most relevant moist processes. MC2 uses semi-Lagranigan advection and a semi-implicit time-differencing dynamical scheme. Because of these schemes, the MC2 model is accurate and efficient. It has proven to be quite versatile as a modeling tool, allowing excellent simulations over a wide spectrum of scales (Benoit et al. 1997), including midlatitude hurricane simulations (McTaggart-Cowan et al. 2001).

We run MC2 with a horizontal resolution of 30 km and with 30 layers in the vertical. The lowest model level is approximately 18 m above the surface. The integration time step is 600 s. Three different model domains are defined for the three storms considered in this study, each with stereographic projection at 60°N. For Earl, the grid is 150 × 142 grid points centered at (42°N, 60°W); for Danielle, 110 × 100 grid points centered at (50°N, 24°W); and for Superbomb, 140 × 140 grid points centered at (41°N, 70°W). Although 30 km is somewhat coarse for tropical hurricane simulations, as it does not properly resolve the eye or eyewall region where surface winds are maximum and where surface fluxes are expected to be most intense, the midlatitude storms considered in this study have sufficiently large horizontal extent so that 30-km resolution gives a good representation of their structure and storm intensity, as shown below. All simulations are initialized using the analysis data generated by the data assimilation system at the Canadian Meteorological Centre (CMC; Chouinard et al. 1994). A force–restore scheme (Benoit et al. 1997) is used for surface heat and moisture fluxes over land. Deep cumulus convection is parameterized using the Kain and Fritsch (1990, 1993) scheme. For each storm, 6-hourly CMC analysis updates are provided at the boundaries. In all simulations, sea surface temperature (SST) is kept the same as the CMC analyses fields although, in reality, variations in temperature and relative humidity at the lowest model level occur as the storms develop.

b. Air–sea flux parameterizations

The key feature of our modeling is that we recognize two routes by which heat and moisture cross the air–sea interface. We refer to the first of these as the interfacial or turbulent fluxes because we use a bulk turbulent flux parameterization to compute them. Whether because the wind is blowing, because the air and sea surface have different temperatures or vapor pressures, or both of the above, the air and sea are always exchanging heat, moisture, and momentum at their interface. The second route by which air–sea fluxes occur is by sea spray. In high winds, sea spray effectively increases the ocean's surface area, thereby enhancing the air–sea fluxes. Our model includes parameterizations for both the interfacial and the sea spray fluxes.

1) BULK TURBULENT FLUX ALGORITHM

The MC2 model computes the interfacial fluxes at the sea surface using a typical bulk turbulent flux algorithm. This predicts the interfacial fluxes of momentum (τ) and sensible (H_s) and latent (H_L) heat from

$$\tau = \rho_a C_D U_{\rm zl}^2, \quad (1)$$

$$H_s = \rho_a c_{\rm pa} C_H U_{\rm zl}(\Theta_0 - \Theta_{\rm zl}), \quad (2)$$

$$H_L = \rho_a L_\upsilon C_E U_{\rm zl}(q_0 - q_{\rm zl}), \quad (3)$$

where positive heat fluxes are upward. Here, U, Θ, and q are the mean wind speed, potential temperature, and specific humidity, respectively; ρ_a is the air density; $c_{\rm pa}$ is the specific heat of air at constant pressure; and L_υ is the latent heat of vaporization of water. Subscript zl denotes the lowest atmospheric model level, and subscript 0 is the ocean surface. The turbulent transfer coefficients for momentum (C_D), sensible heat (C_H), and latent heat (C_E) in Eqs. (1)–(3) derive from Monin–Obukhov similarity theory and are often predicted from the roughness lengths for wind speed (z_{0m}), temperature (z_{0t}), and humidity (z_{0q}; Fairall et al. 1996).

Because the MC2 model has default parameterizations for z_{0m}, z_{0t}, and z_{0q}, we must exercise some care regarding these defaults because Andreas (2003) developed the bulk spray flux algorithm we use by subtracting estimates of the interfacial heat fluxes from HEXOS measurements of the total heat fluxes. In other words, what is left is the spray flux; consequently, his spray algorithm is tuned to a specific turbulent bulk flux algorithm. The spray algorithm may not be valid if we use it with a different bulk flux algorithm. Therefore, in the spray algorithm, we ignore MC2's default bulk flux algorithm and implement the parameterizations that Andreas (2003) used in his HEXOS analysis. To estimate z_{0m}, we set

$$z_{0m} = 0.135\frac{\nu}{u_*} + 0.0185\frac{u_*^2}{g}, \quad (4)$$

where ν is the kinematic viscosity of air, g is the acceleration of gravity, and u_* [$=(\tau/\rho_{\rm a})^{1/2}$] is the friction velocity. Here z_{0m} is in meters when the other quantities in Eq. (4) are in mks units. Equation (4) derives from Smith (1988) and is also in the Tropical Ocean Global Atmosphere Coupled Ocean–Atmosphere Response Experiment (TOGA COARE) algorithm (Fairall et al. 1996), though with a smaller value for the Charnock constant than 0.0185. Our value is appropriate for the rougher seas under the storms we are simulating (e.g., Wu 1982; Johnson et al. 1998). Coincidentally, the corresponding default MC2 parameterization for z_{0m} is given by Eq. (4), but without the first term on the right-hand side, and with the Charnock constant set to 0.0180, which is a negligible difference since that first term is significant only in very low winds.

For z_{0t} and z_{0q} in the spray algorithm, we use the parameterization of Liu et al. (1979), which is also the basis for the TOGA COARE version 2.6 algorithm (Fairall et al. 1996). The MC2 model, on the other hand, assumes that z_{0t} and z_{0q} both equal z_{0m}, typical of atmospheric models uncoupled to the upper ocean (see, e.g., Emanuel 1995), and would thus predict larger interfacial sensible and latent heat fluxes that would be incompatible with the spray flux algorithm. Because the Liu et al. parameterization and Eq. (4) predict z_{0t} and z_{0q} values that are smaller than the mean free path of air molecules when u_* exceeds 0.88 m s^{-1} (=1.71 kt), we limit z_{0t} and z_{0q} to values greater than or equal to 7.0×10^{-8} m, the typical mean free path in air.

We follow the usual iterative approach to solving Eqs. (1)–(3) for the interfacial fluxes. In the first step, we assume neutral stability and use Large and Pond's (1981) formulation for the drag coefficient as a function of wind speed to make first estimates of the friction velocity u_* and the turbulent heat fluxes. Having these, we can 1) estimate the stability; 2) compute z_{0m} [from Eq. (4)], z_{0t}, and z_{0q}; 3) then compute better values of the transfer coefficients in Eqs. (1)–(3); and 4) thereby, revise our flux estimates. We continue this iteration until all three turbulent fluxes converge, which takes only about five iterations.

2) Spray flux algorithm

Spray droplets ranging in initial radius from about 1 to 500 μm carry essentially all of the spray heat and moisture across the air–sea interface. Andreas and DeCosmo (1999, 2002) used a sophisticated microphysical model and a spray generation function that models the production rates of all these droplets when they identified a spray flux signature in the eddy-correlation data from HEXOS. We cannot afford such a computationally intensive model in our storm simulations here.

However, computations with Andreas's (1992) spray flux model suggest that droplets whose initial radii are around 100 μm carry most of the spray sensible heat, and droplets with initial radii around 50 μm carry most of the spray latent heat (Andreas 1992, 1998; Andreas et al. 1995). Andreas (2003) therefore assumed that these droplets are the bellwethers of the respective spray fluxes and consequently modeled the spray sensible heat flux as

$$Q_{s,\rm sp} = \rho_w c_w(\Theta_{\rm o} - T_{\rm eq,100})V_s(u_*), \quad (5)$$

and the spray latent heat flux as

$$Q_{L,\rm sp} = \rho_w L_\upsilon\left[1 - \left(\frac{r_{\rm eq,50}}{50\ \mu m}\right)^3\right]V_L(u_*). \quad (6)$$

In these expressions, ρ_w is the density of seawater; c_w, the specific heat of seawater; $T_{\rm eq,100}$, the equilibrium or evaporating temperature of spray droplets with initial radius 100 μm; and $r_{\rm eq,50}$, the equilibrium radius of droplets that are initially 50 μm in radius.

Finally, the wind functions V_s and V_L depend on u_* and tune Eqs. (5) and (6) to data. Many sources suggest that spray generation is proportional to the cube of the wind speed or the cube of u_* (see Andreas 2002 for a review). Andreas and Emanuel (2001) therefore fitted an equation similar to Eq. (5) with a wind speed function that is cubic in u_*. Andreas (2003) likewise fitted

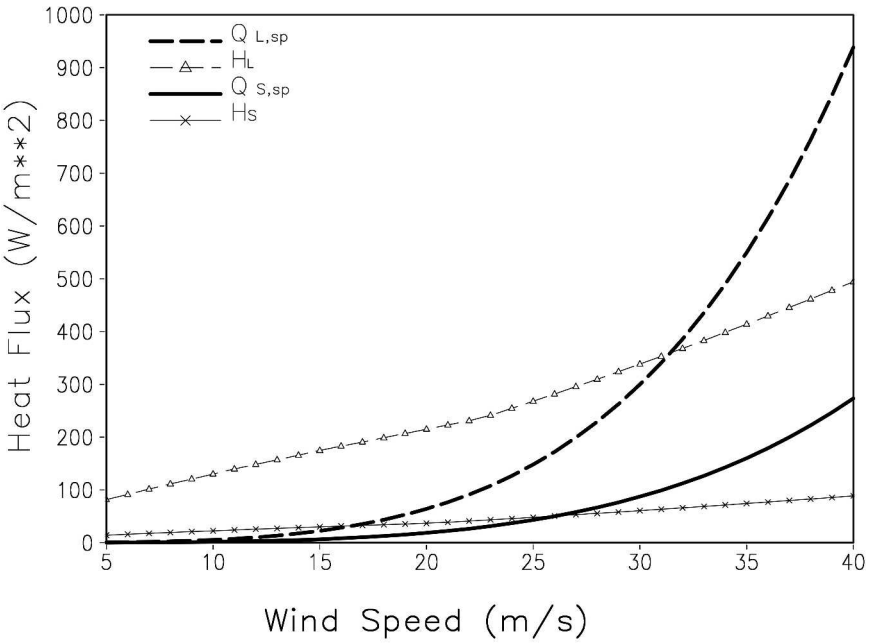

FIG. 1. Magnitude of the interfacial (H_s, H_L) and spray-mediated ($Q_{s,\mathrm{sp}}$, $Q_{L,\mathrm{sp}}$) sensible and latent heat fluxes as a function of wind speed, assuming 80% relative humidity, a salinity of 35 psu, a central SLP of 980 mb, an air temperature of 15°C, and SST of 17°C.

HEXOS data analyzed according to Eqs. (5) and (6) with V_s and V_L functions modeled as cubics in u_*. His results are

$$V_s(u_*) = 1.65 \times 10^{-6}\, u_*^3, \tag{7}$$

$$V_L(u_*) = 4.75 \times 10^{-8}\, u_*^3. \tag{8}$$

Units for $Q_{s,\mathrm{sp}}$ and $Q_{L,\mathrm{sp}}$ in Eqs. (5) and (6), as well as for H_s and H_L in Eqs. (2) and (3), are W m^{-2} when u_* is in m s^{-1}. Equations (5)–(8) thus constitute our spray flux parameterization.

3) COMBINED FLUXES

The combined spray and interfacial fluxes constitute the boundary conditions at our lowest model level. We simply add the heat fluxes together to get the total sensible ($H_{s,T}$) and latent ($H_{L,T}$) heat fluxes:

$$H_{s,T} = H_s + Q_{s,\mathrm{sp}}, \tag{9}$$

$$H_{L,T} = H_L + Q_{L,\mathrm{sp}}. \tag{10}$$

During this study, we realized that the spray flux algorithm, Eqs. (5)–(10), has some shortcomings (Li et al. 2003). Most notably, the formulation for $Q_{L,\mathrm{sp}}$ depends too weakly on temperature. Computations with Andreas's full microphysical spray model (e.g., Andreas 1990, 1992; Andreas et al. 1995) show that the spray latent heat flux increases dramatically as the air temperature increases. Basically, droplets evaporate more rapidly in warmer air than in cooler air. Because $r_{\mathrm{eq},50}$ depends very weakly on temperature, however, Eq. (6) cannot reproduce this behavior and will thus overestimate the spray latent heat flux when it is used in conditions much cooler than conditions for which it was tuned. Conversely, Eq. (6) will underestimate the spray latent heat flux in much warmer conditions.

Fortunately, in this study of extratropical storms, we are using the spray flux algorithm in temperatures near those for which it was tuned. Andreas (2003; also Andreas and DeCosmo 2002) tuned the spray flux algorithm with HEXOS data obtained over the North Sea in the fall (DeCosmo 1991; DeCosmo et al. 1996). Sea surface temperatures in this dataset were between 9.8°and 14.9°C. Since these surface temperatures are comparable to those in the storms we simulate, we are using the spray algorithm within the domain for which it should be most accurate.

4) VARIATION AS A FUNCTION OF WIND SPEED

To get an indication of the magnitude of the spray-mediated fluxes, we plot estimates of H_s, H_L, $Q_{S,\mathrm{sp}}$, and $Q_{L,\mathrm{sp}}$ as functions of wind speed at 18 m (the lowest MC2 model level in this study) in Fig. 1. This level is above the droplet evaporation layer, where spray processes are most active. The maximum wind speeds in Fig. 1 are approximately the maxima seen in extratropical hurricanes in the northwest Atlantic. Figure 1 shows that the spray-mediated latent heat flux increases much more rapidly with wind speed than the interfacial fluxes, supporting the suggestion that the latent heat flux rather than the sensible heat flux is the key influ-

ence of sea spray on hurricanes. Above 30 m s^{-1}, the approximate hurricane threshold wind speed, $Q_{L,\mathrm{sp}}$ exceeds H_L and increases rapidly with increasing winds. However, a caveat is that HEXOS data are able to verify only the portion of this figure with speeds less than 20 m s^{-1} (i.e., Andreas and DeCosmo 2002).

3. Storm cases

While most studies that deal with the impact of sea spray focus on tropical cyclones (Kepert et al. 1999; Bao et al. 2000; Wang et al. 2001), we consider three midlatitude storms.

a. Ex-Hurricane Earl (1998): Extratropical transition

Tropical Storm Earl formed 930 km south-southwest of New Orleans at 1800 UTC 31 August and subsequently reached hurricane status 230 km south-southwest of New Orleans at 1200 UTC 2 September. The storm thereafter rapidly intensified to category 2 (winds in excess of 42 m s^{-1}) and made landfall near Panama City, Florida, as a category-1 hurricane at 0600 UTC 3 September. The system continued its northeasterly track across the Carolinas and continued to fill. Exiting the continental United States north of Cape Hatteras just after 1200 UTC 4 September, the storm lay 350 km off the New Jersey coastline by 0000 UTC 5 September with a central sea level pressure (SLP) of 1000 mb.

The subsequent 36 h saw ex-hurricane Earl declared extratropical by the National Hurricane Center (NHC) at 1800 UTC 3 September, when it reintensified to 964 mb in the waters off the Canadian Maritime provinces. A strong midlevel trough interacted with the system over this period, causing a rapid spinup of the lower-level vortex as midlatitude forcings combined with the latent energy contained within the moist tropical air near Earl's center. A cyclonic vortex rollup was observed during reintensification, suggesting that baroclinic processes were still prevalent over the period. At 1200 UTC 6 September, Earl made a sharp anticyclonic track change, thus completing recurvature, and accelerated to the eastern North Atlantic, where it merged with remnants of Danielle (McTaggart-Cowan et al. 2001).

b. Ex-Hurricane Danielle (1998): Extratropical transition

Danielle reached hurricane status on 25 August in the central Atlantic. Subsequently, it reached two intensity maxima during 26–27 August (McTaggart-Cowan 2003), both exceeding category-2 storm intensity, as it traveled westward across the equatorial Atlantic. Danielle tracked slowly northeastward, coming within 850 km of Florida and recurving to take a northeasterly track off the eastern seaboard, partially following Bonnie's cool wake. At 1200 UTC 31 August, it reached a third intensity maximum of 45 m s^{-1} and, accelerating parallel to the coast, a fourth intensity maximum (again 45 m s^{-1}) with a central sea level pressure of 965 mb at 1800 UTC 1 September. Declared extratropical at 0000 UTC 4 September by NHC, Danielle took an easterly track beneath a strong midlevel steering flow until 0000 UTC 5 September, with an estimated central pressure of 975 mb.

Over the subsequent 30 h, the system intensified to 964 mb. A weak midlevel trough was likely responsible for triggering deep convection, which dominated the reintensification thereafter. The resulting system was remarkably symmetric and lacked identifiable frontal features in satellite imagery. Using this observation, combined with dynamic tropopause analyses, McTaggart-Cowan et al. (2004) designated this a tropical mode reintensification. The rejuvenated system tracked slowly northeastward until 8 September and merged with a preexisting extratropical structure and remnants of Earl.

c. Superbomb (2000): Rapid oceanic cyclogenesis

Superbomb is one of a series of winter storms that track along the North American east coast. On 20 January, the CMC analysis placed a surface center with a reduced sea level pressure of 1006 mb in southern Illinois. Over the following 12 h, westerly flow to the south of the circulation center began to feel the warm (20°–24°C) coastal waters south of Cape Hatteras. Exiting the coast, the system's circulation quickly extended southeastward as the 4°C destabilizing air wrapped rapidly around it. A secondary center superposed on a warm (>24°C) Gulf Stream eddy amid warm localized mixed-layer temperatures resulted in cyclogenesis and absorption of the original circulation center by the incipient marine system.

The newly formed center tracked rapidly northeastward parallel to the coast from 1200 UTC 20 January to 1200 UTC 21 January, deepening from 997 to 955 mb (Figs. 2c, 4e). This motivates the moniker "Superbomb" because it deepened much more rapidly than a typical "bomb" (defined as having a central pressure that falls by a rate of least 1 mb h^{-1} for 24 h; Sanders and Gyakum 1980; Glickman 2000, p. 93). At midlevels, a short wave traveled quickly around the base of a deepening larger-scale trough centered over Hudson Bay. This, combined with continued convective activity in the destabilized air off the coast, contributed to the formation of a cutoff flow at 500 mb over Sable Island at 1200 UTC 21 January. The system was still under the influence of a linear jet to its south and west, thus benefiting from the divergent upper-level forcing associated with the left-exit region. Phase locking occurred shortly after this time, and the vertically stacked system began to curl northward under the influence of the flow at midlevels. The rate of intensification leveled off, and the central pressure remained at 956 mb until

0000 UTC 22 January. The system made landfall in Cape Breton shortly before 0000 UTC 22 January and tracked northwestward to the Gulf of St. Lawrence as the central pressure weakened to 972 mb. Filling continued as it moved toward its Baffin Bay cyclolysis region.

4. Sea spray impacts

While Superbomb experienced explosive intensification (see Kuo et al. 1991), the two transitioning systems, Danielle and Earl, underwent tropical and baroclinic modes of extratropical transition, respectively (see McTaggart-Cowan et al. 2004). The redevelopment of Earl's circulation occurred primarily because of large-scale (life cycles) LC-2-type baroclinic processes that resulted in strong frontal features (Thorncroft et al. 1993). In Danielle's case, the tropical forcings played an enhanced role in the reintensification, as warm, moist air was advected northward in a broad region ahead of the cyclone and created a local environment almost devoid of thermal gradients and with a uniformly low bulk convective stability (McTaggart-Cowan et al. 2004). We therefore expect near-surface physical processes to more greatly impact Danielle than Earl since atmospheric boundary layer modifications can strongly affect lower-level stability.

a. Storm track

Figure 2 compares the storm tracks of Earl, Danielle, and Superbomb for simulations with and without sea spray and show that the simulated tracks are close to the NHC analysis (or CMC analysis in Superbomb). In each storm case, the decelerating storm speed is well modeled, as is the increasing northward component of each storm's trajectory. The setup and execution of the control simulation for Earl is virtually identical to that of McTaggart-Cowan et al. (2001). Slight changes in simulated storm tracks are evident in Fig. 2 because of the impact of spray on air–sea heat fluxes and storm development.

As further verification that MC2 gives good baseline simulations of storms, Fig. 3 compares the MC2 wind fields at Superbomb's peak and the QuikSCAT–NCEP (National Centers for Environmental Prediction) merged wind fields (available online at http://dss.ucar.edu/datasets/ds744.4/), for 0600 UTC 21 January 2000. The overall structures of the QuikSCAT–NCEP merged wind field and the MC2 wind field are quite similar. Both estimate the same storm center at approximately (41°N, 66°W). While QuikSCAT–NCEP estimates suggest that the maximum wind speed is 42 m s^{-1}, the MC2 model estimate is 41 m s^{-1}. Sea spray is not included in this MC2 simulation.

b. Storm intensity

While the overall impact of sea spray on storm tracks is small, spray's impact on storm intensity and development differs for the three storms. These differences reflect different wind speeds, SSTs, and storm propagation speeds, which influence the spray-mediated heat fluxes and, in turn, modify the storm's life cycle. For example, although Earl and Danielle made transitions to extratropical hurricanes with significant intensifica-

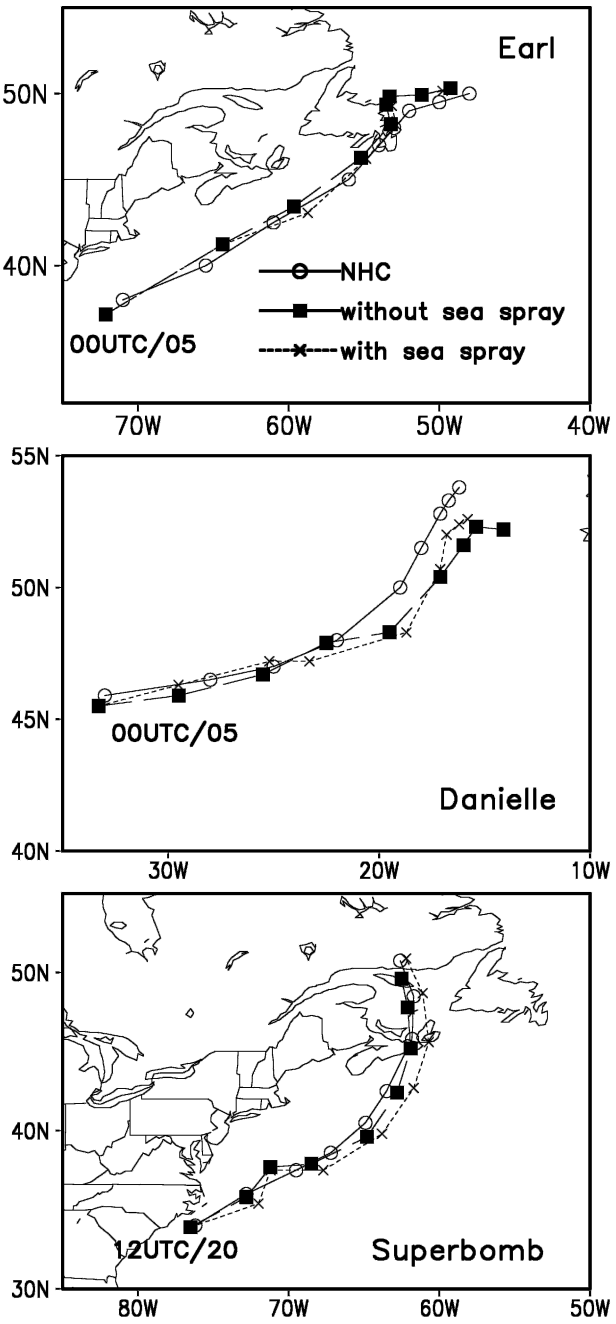

FIG. 2. Comparisons of analyzed and simulated storm tracks of Hurricanes (a) Earl and (b) Danielle and (c) Superbomb, with and without sea spray. Storm center locations are plotted every 6 h. Simulations for Earl and Danielle begin at 0000 UTC 5 Sep 1998. Simulations for Superbomb begin at 1200 UTC 20 Jan 2000. Times and dates are indicated for the CMC results in each panel.

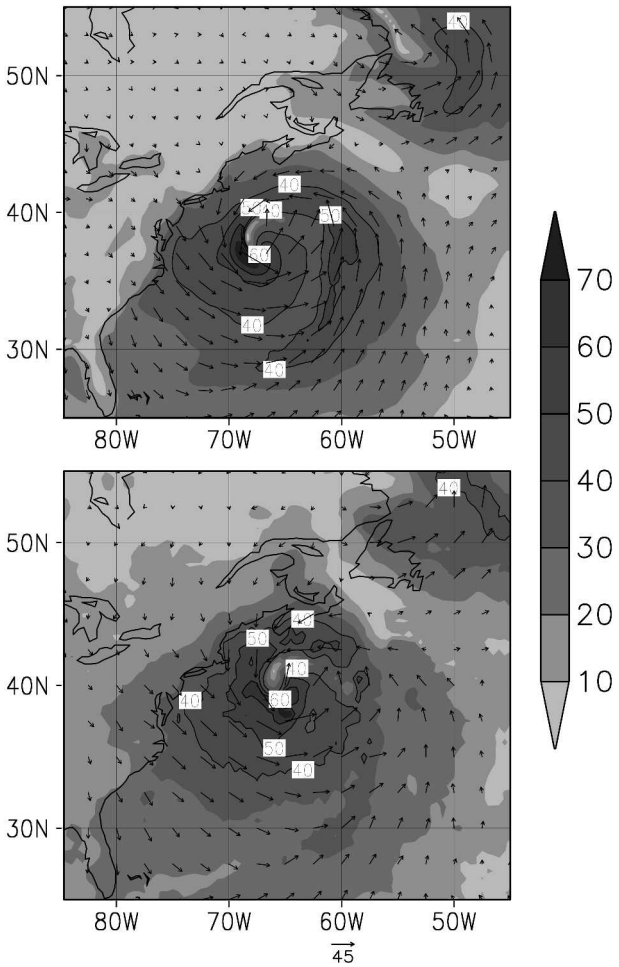

FIG. 3. Comparison of (a) MC2 simulation, without sea spray, at the peak wind field (kt) of Superbomb to (b) QuikSCAT–NCEP blended wind fields. Both plots are at 0600 UTC 21 Jan 2000, with the storm center at approximately (41°N, 66°W).

tion, Earl's maximum 10-m wind speed, U_{10}, was 44 kt, whereas Danielle's was 55 kt in our MC2 simulations (below Figs. 4b,d). These winds were obtained by averaging over an area of 200^2 km^2 that covered the high-wind region of the simulations of each storm. The storm tracks differ in that Earl's SSTs range from 25°C in the south to 5°C in the north, whereas Danielle's range from 20°C to 15°C. By comparison, Superbomb's (area averaged) winds achieved 60 kt, and SSTs ranged from Cape Hatteras waters (20°C) to the cool Gulf of St. Lawrence (0°C).

In Fig. 4, we give the minimum central sea level pressure and maximum (area averaged) 10-m wind speed (U_{10}) from simulations with and without sea spray for the three storms as they propagate along their respective storm tracks. For Earl, the (control) simulated intensity compares well with analyzed sea level pressure data. The central pressure (Fig. 4a) falls to 967 mb after 36 h of simulation and is comparable with both NHC and CMC analyses at 1200 UTC 6 September. Despite initial differences, the model simulations, with and without spray, are both within 4 mb of the analyzed minimum pressure for the duration of the integration. The U_{10} winds in the NHC and CMC analyses (Fig. 4b) qualitatively agree with our simulations during Earl's reintensification phase (0–36 h). The maximum difference between U_{10} in the spray and no-spray simulations is only about 4.8 kt, which is about the resolution of the NHC analysis interval (5.0 kt) and is much less than the difference between NHC and CMC analyses.

In Danielle, spray impacts are larger than those of Earl because of the higher winds: Maximum changes in central pressure and U_{10} are 2 mb and 7.3 kt, respectively; and the MC2 spray simulation achieves (area averaged) winds of 62.7 kt (Figs. 4c,d). However, the U_{10} change is slightly larger than the resolution of the NHC analysis interval and much less than the difference between NHC and CMC analysis results. As in Earl, despite disagreement between the 0000 UTC 5 September NHC analysis and our initial sea level pressure fields, our simulations produce stronger storms than the NHC or CMC analyses suggest in terms of central pressure; the intensification period in the simulations, though, is similar to those of the NHC and CMC analyses.

Finally, Superbomb (Figs. 4e,f) is the strongest of the three storms. Both MC2 control and MC2 spray simulations capture the *initial* CMC analysis central sea level pressure well. Subsequent storm tracks and development from both simulations are consistent with the CMC analysis. The MC2 spray simulation achieves maximum (area averaged) wind speeds of 70 kt and suggests enhanced deepening of the central pressure by 5 mb and higher U_{10} by 10 kt compared to the MC2 control run. By comparison, the QuikSCAT–NCEP merged estimate of maximum wind speed for the storm peak is 81 kt (see online at http://dss.ucar.edu/datasets/ds744.4/). Therefore, the MC2 spray simulation shows an overall improvement, compared to MC2 control, in simulating U_{10} during the storm's decay phase (1200 UTC 21 January–1200 UTC 22 January).

Figure 5 compares simulations with and without sea spray for the three storms, showing winds (U_{10}), wind speed differences (ΔU_{10}), and sea level pressure differences (ΔSLP) when the latter is maximal. In each case, sea spray proliferates within a few hours after the simulations begin and ultimately deepens the central pressure over the cyclone region by ~2 mb for Earl, ~3 mb for Danielle, and ~6 mb for Superbomb, with related U_{10} increases. Moreover, spray slightly perturbs the storm tracks, compared to MC2 control simulations, to the extent that slight dipole contour features may appear in central pressure fields (e.g., as in Danielle in Fig. 5b2). These results are consistent with Kuo et al. (1991), suggesting that if latent heating effects are implemented in the very early stages of the storm de-

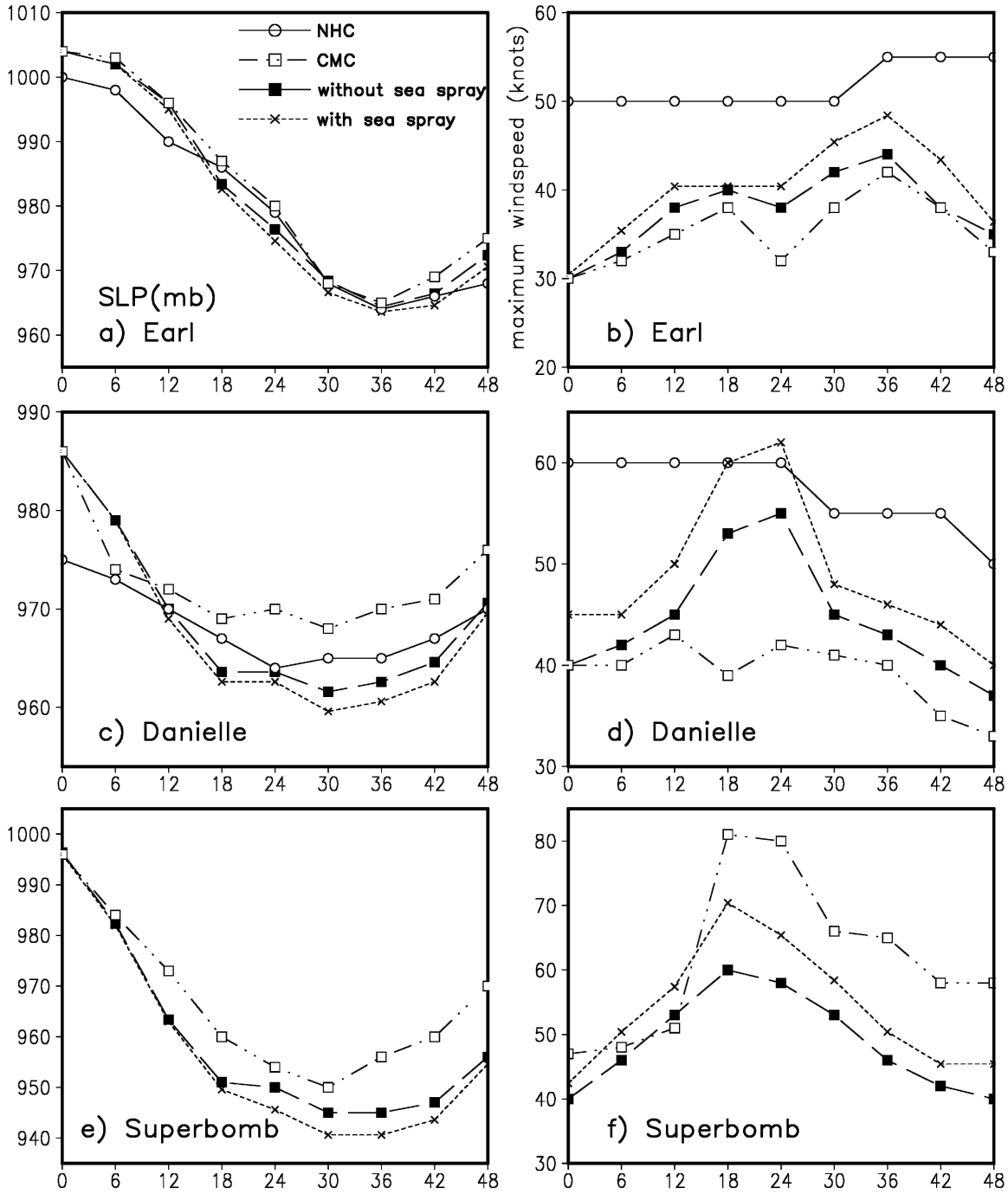

FIG. 4. Time series of central SLP and maximum (area averaged) 10-m winds for (a), (b) Earl, (c), (d) Danielle, and (e), (f) Superbomb. Area averages are computed on 200^2 km^2 covering the high-wind region of each storm.

velopment, preceding rapid intensification, they can significantly influence storm intensification.

c. Surface fluxes

The regions of greatest sea spray contribution to the heat fluxes are near the center of the storm and propagate with the storm as it develops. Figure 6 gives time series for the maximum latent and sensible heat fluxes following the respective storm tracks, area averaged (300^2 km^2) about the center of each storm. While spray enhances both sensible and latent heat fluxes, the effect is most important on latent heat fluxes. In each storm, the maximum latent heat flux approximately coincides with the U_{10} maximum, and the maximum spray impact on the storm reflects the storm intensity; about

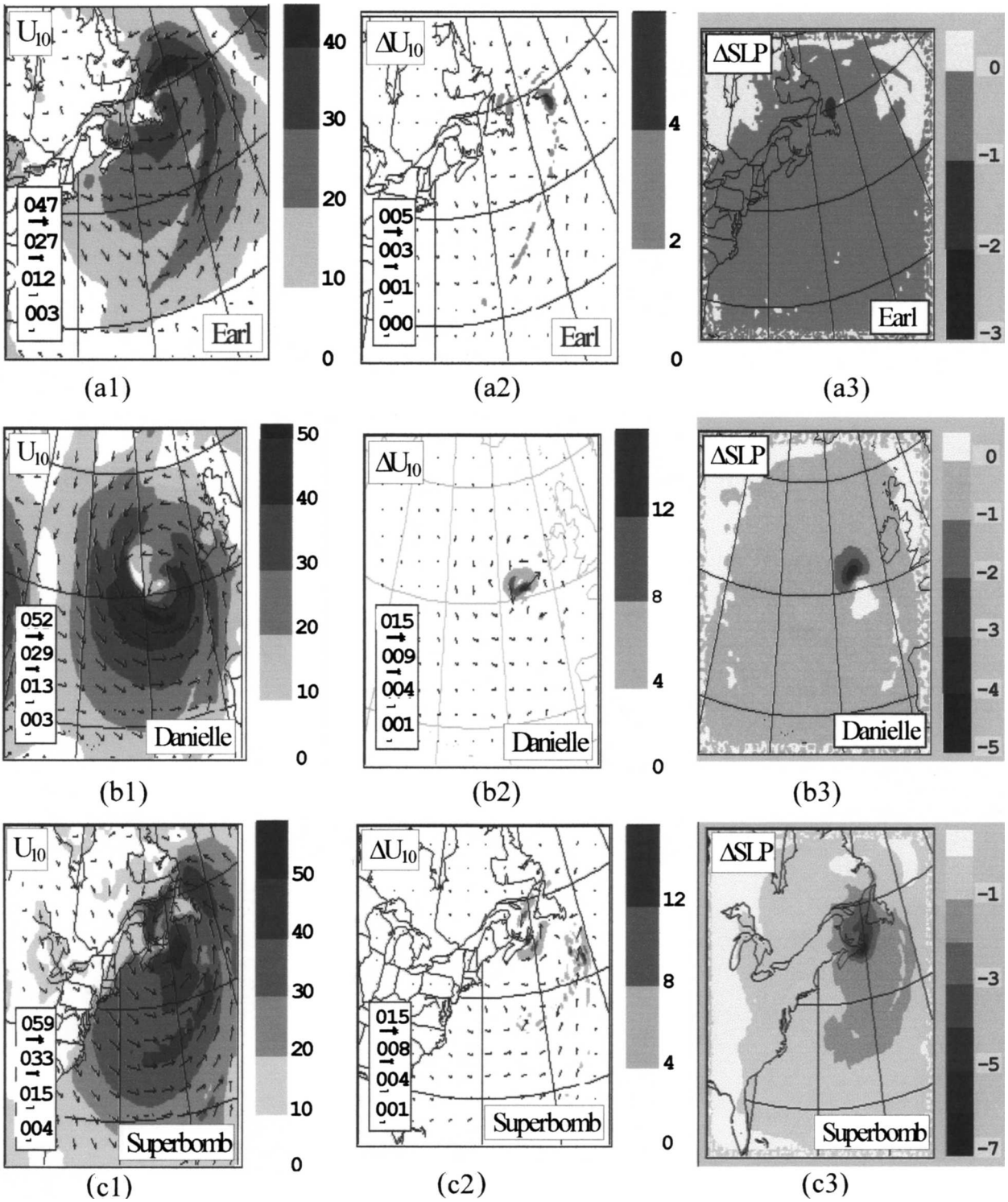

FIG. 5. Winds (U_{10} in kt from the spray simulation), wind speed differences ΔU_{10}, and ΔSLP (mb) for simulations with spray *minus* simulations without spray for (a1), (a2), (a3) Earl at 0600 UTC 6 Sep; (b1), (b2), (b3) Danielle at 0600 UTC 6 Sep; and (c1), (c2), (c3) Superbomb at 0000 UTC 22 Jan. In each case, at these times, ΔSLP was *maximal* for each storm for the simulations with and without spray.

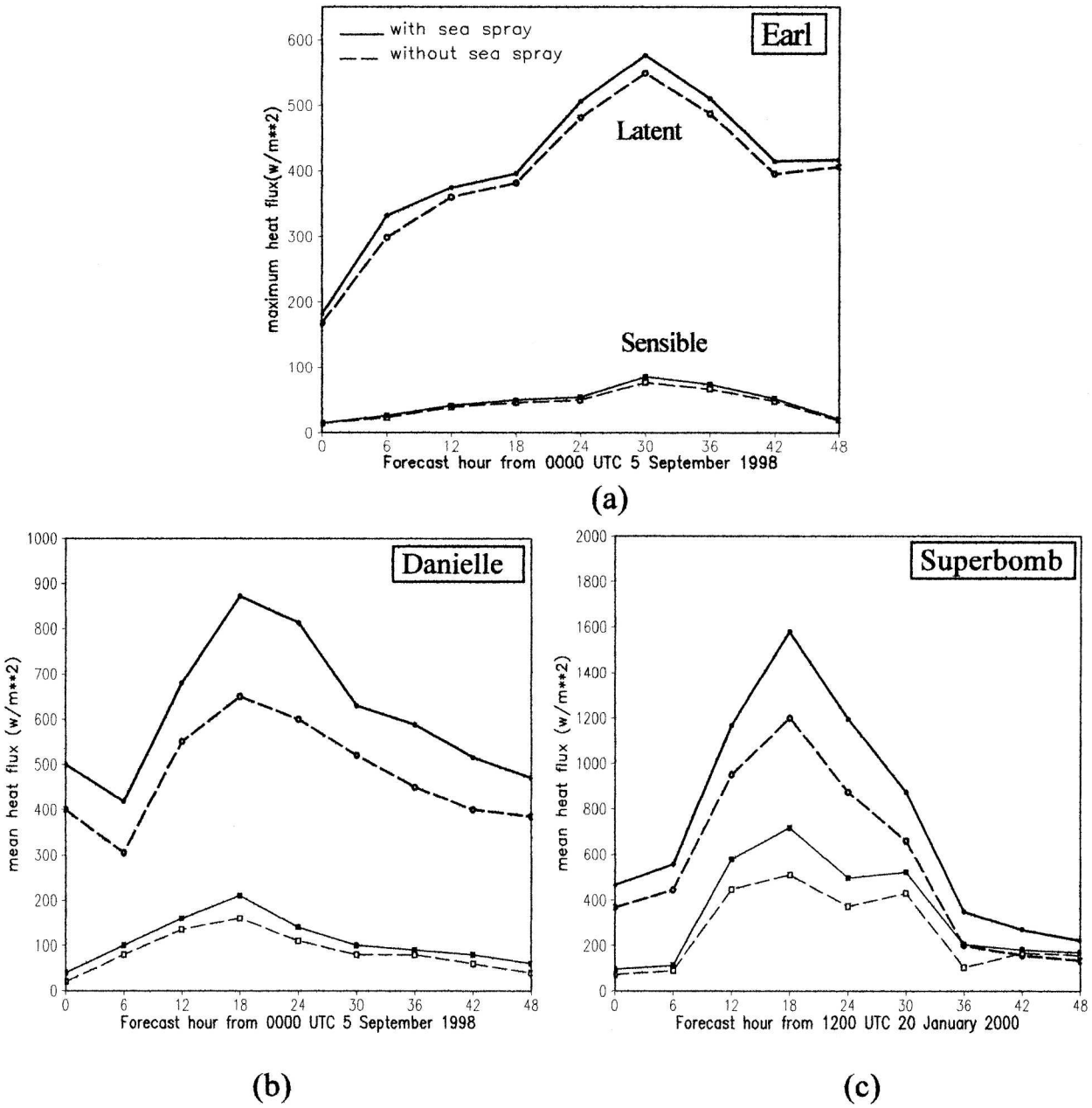

FIG. 6. Time series (area averaged) of maximum latent and sensible heat fluxes from simulations with and without sea spray, following the storm track, for (a) Earl, (b) Danielle, and (c) Superbomb. In each case, the thick (upper) solid line is the latent heat flux with spray, and the thick (upper) dashed line is the latent heat flux without spray; the thin (lower) solid line is the sensible heat flux with spray, and the thin (lower) dashed line is the sensible heat flux without sea spray. Area averages consist of 300^2 km^2 centered at the minimum SLP.

25 W m^{-2} for Earl, 230 W m^{-2} for Danielle, and 375 W m^{-2} for Superbomb. The maximum spray impact on sensible heat flux was smaller; about 10 W m^{-2} for Earl, 50 W m^{-2} for Danielle, and 190 W m^{-2} for Superbomb. Figure 7 shows U_{10} fields and the coincident *differences* in latent heat fluxes between MC2 control and MC2 spray results for Danielle and Superbomb, at the time when latent heat fluxes are maximal in Figs. 6b and 6c. These plots show the spatial distribution and strength of spray-induced latent heat flux impacts, reflecting Danielle's relatively large spatial extent compared to Superbomb's smaller extent and higher intensity.

d. Marine boundary layer structure

All three storms in this study have very asymmetric wind fields (Figs. 5a1, 5b1, 5c1), which change and

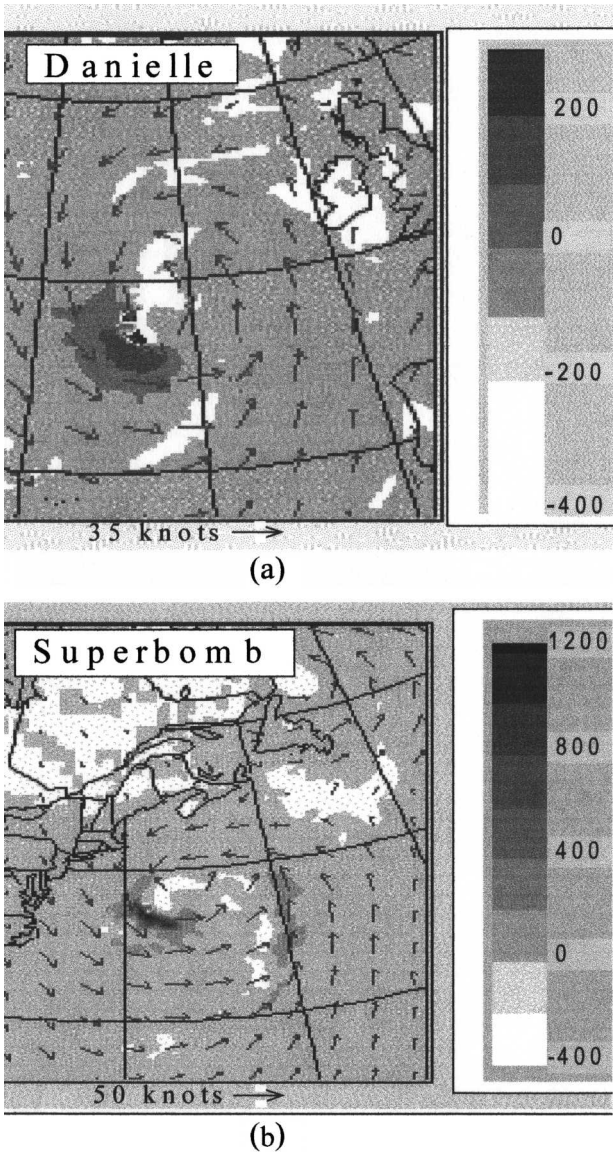

FIG. 7. *Differences* in latent heat fluxes (at the peaks in Figs. 6b, c; W m^{-2}) for simulations with spray *minus* simulations without spray: (a) Danielle at 1800 UTC 5 Sep, (b) Superbomb at 0600 UTC 21 Jan 2000. Wind speed vectors (kt) are also shown.

evolve as the storm develops and intensifies. Although heat fluxes associated with the spray exhibit spatial modifications, these modifications diminish with increasing height. In Fig. 8, we show the Superbomb 1000–500-mb thickness, *h,* and sea level pressure contours for MC2 control and MC2 spray simulations corresponding to the time (0000 UTC 22 January) when spray impacts on surface pressure are maximum (as given in Figs. 5c1–3). Although Superbomb is the strongest of the three storms, spray results in only a very small increase in *h* and a moderate decrease in SLP (~5 mb).

Figure 9 shows the vertical profiles for spray impacts on maximum wind speeds by comparing differences between MC2 control and MC2 spray simulations for the three storms. The figure shows that the effects of spray are predominantly confined to the lowest 2000 m and tend to peak at about 800 mb. These differences are 4 kt for Earl, 8 kt for Danielle, and 12 kt for Superbomb. These values were obtained by averaging (200^2 km^2) around the maximum wind speed contour. At upper levels, above about 500 mb, the impact of spray is negligible.

Related to the spray impacts on the vertical wind profile are its more direct effects on temperature and humidity, which reflect the moisture flux into the marine boundary layer. Figure 10 shows vertical profiles for differences in temperature ΔT and specific humidity Δq between MC2 control and MC2 spray runs. While Superbomb shows an enhanced spray impact on specific humidity of 1.4×10^{-3} kg kg^{-1}, impacts for Danielle and Earl are progressively weaker. For all three storms, spray humidity effects are negligible above 700 mb. The corresponding temperature effect is that, at the storm center, sea spray reduces the surface and low-level temperatures due to droplet evaporation and warms a higher level at about 500–700 mb. The latter is a dynamic response, such as a change in the secondary circulation, to accommodate the strong latent heat release associated with recondensing spray-derived vapor around 800 mb and altered frictional forcing, as could be explained by a balanced vortex model.

The physical explanation of this is that the spray droplets take heat from the atmospheric boundary layer to evaporate. That is, the spray-induced latent heat flux acts as a sink for boundary layer sensible heat. The maximum low-level cooling and higher-level warming for Earl are approximately −0.3° and +0.3°C; for Danielle, −0.6° and +0.4°C; and for Superbomb, −1.5° and +1.0°C, respectively (Figs. 10a,c,e). Thus, each storm's stratification is essentially unstable, and heat fluxes are upward from the ocean. Latent and sensible heat fluxes are enhanced in the spray simulations and create cooler, moister atmospheric boundary layers, also shown in Fig. 6. Particularly at the lowest model levels, enhanced moisture flux and evaporation result in lower temperatures, which in turn enhance the interfacial sensible heat flux from the ocean surface.

Vertical profiles for equivalent potential temperature θ_e show the essential storm signatures (Fig. 11): a rather homogeneous θ_e chimney extending from the ocean surface almost to the midtroposphere and reflecting the slanting structures of the storms. For Earl, Danielle, and Superbomb, the θ_e chimneys indicate storm centers at 304.8°, 340°, and 291.5°, respectively. The impacts of sea spray are given by the difference profiles, $\Delta\theta_e$, for simulations with spray minus those without spray. In each storm case, the storm center is again indicated by the peak negative, vertically slanting $\Delta\theta_e$ contours, which have values of −2, −2, and −1 K, respectively.

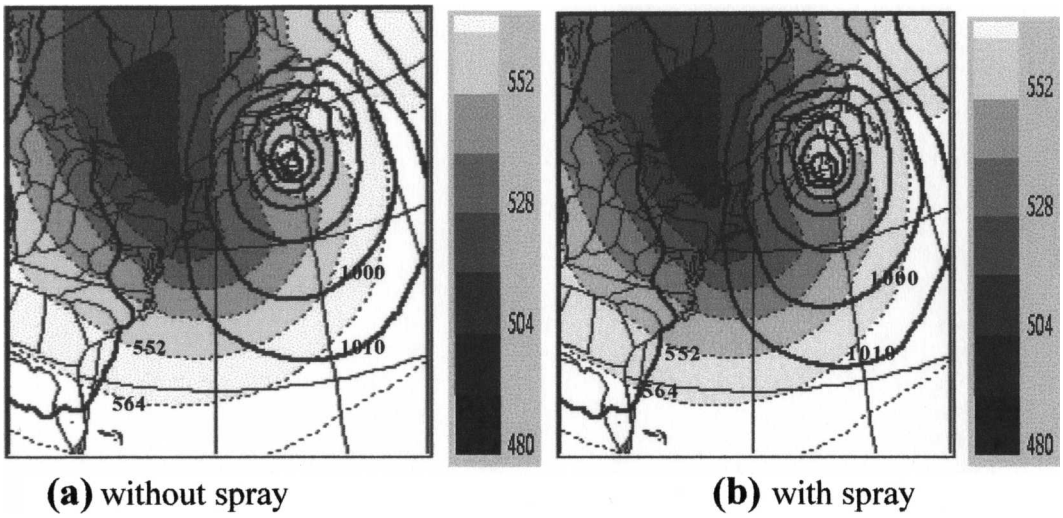

FIG. 8. The 1000–500-mb thickness, h, (shaded dashed contours, units are in dam) and SLP (solid contours, units are mb) for Superbomb at 0000 UTC 22 Jan, when spray impacts on surface pressure are maximum (as in Figs. 5c1–3). Contour increments for h and pressure are 12 m and 10 mb, respectively. With sea spray, maximum h is 549 m and minimum pressure is 941 mb, and without sea spray, 547 m and 946 mb.

Corresponding positive $\Delta\theta_e$ contours tend to occur on either side, as shown in the longitude–height sections. An explanation for the latter is that because the SST field is fixed in time during our simulations, the cooler air temperature (T_a) near the storm center causes an increased difference between SST and T_a values, and, hence, an increase in the sensible heat flux. The enhanced sensible heat flux is redistributed within the boundary layer providing a mechanism for the positive $\Delta\theta_e$ contours outside the storm center. Thus, positive and negative $\Delta\theta_e$ contours due to the impact of spray tend to deepen the positive–negative–positive gradients defining the θ_e chimney and, thus, to intensify the storm. Moistening, boundary layer cooling from droplet evaporation, and enhanced sensible heat flux from the ocean are given by the results in the $\Delta\theta_e$ longitude–height sections in Fig. 11. These show the centers of the storms when the winds are maximal (see Figs. 9–10).

A dominant factor in determining the negative contours of $\Delta\theta_e$ is the temperature depression ΔT in com-

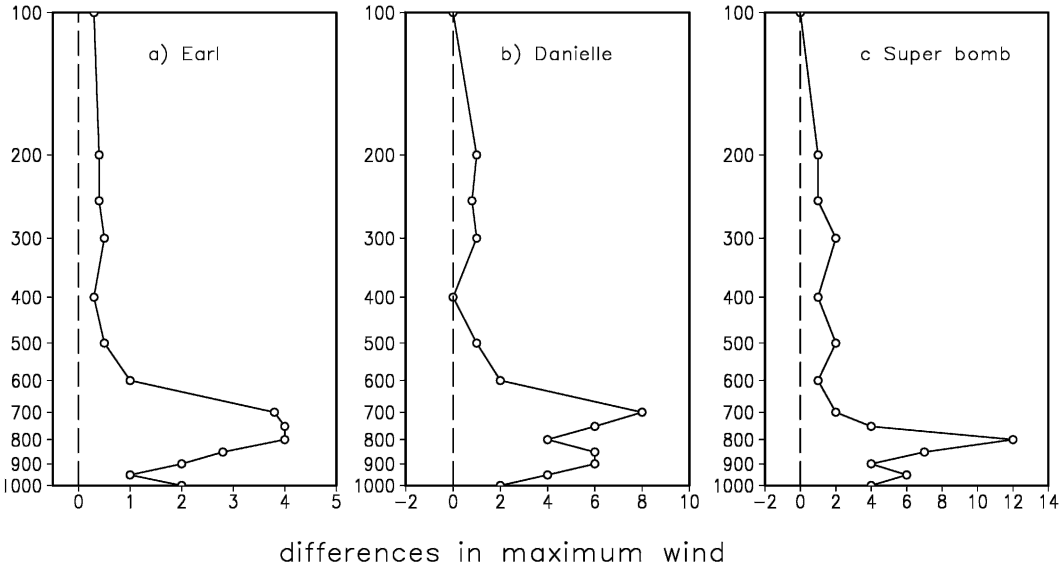

FIG. 9. Vertical profile of differences in maximum wind speed (kt) for simulations with spray *minus* simulations without spray for (a) Earl at 1800 UTC 5 Sep, (b) Danielle at 0000 UTC 6 Sep, and (c) Superbomb at 0600 UTC 21 Jan. All profiles are (200^2 km^2) area averages about the maximal U_{10} region.

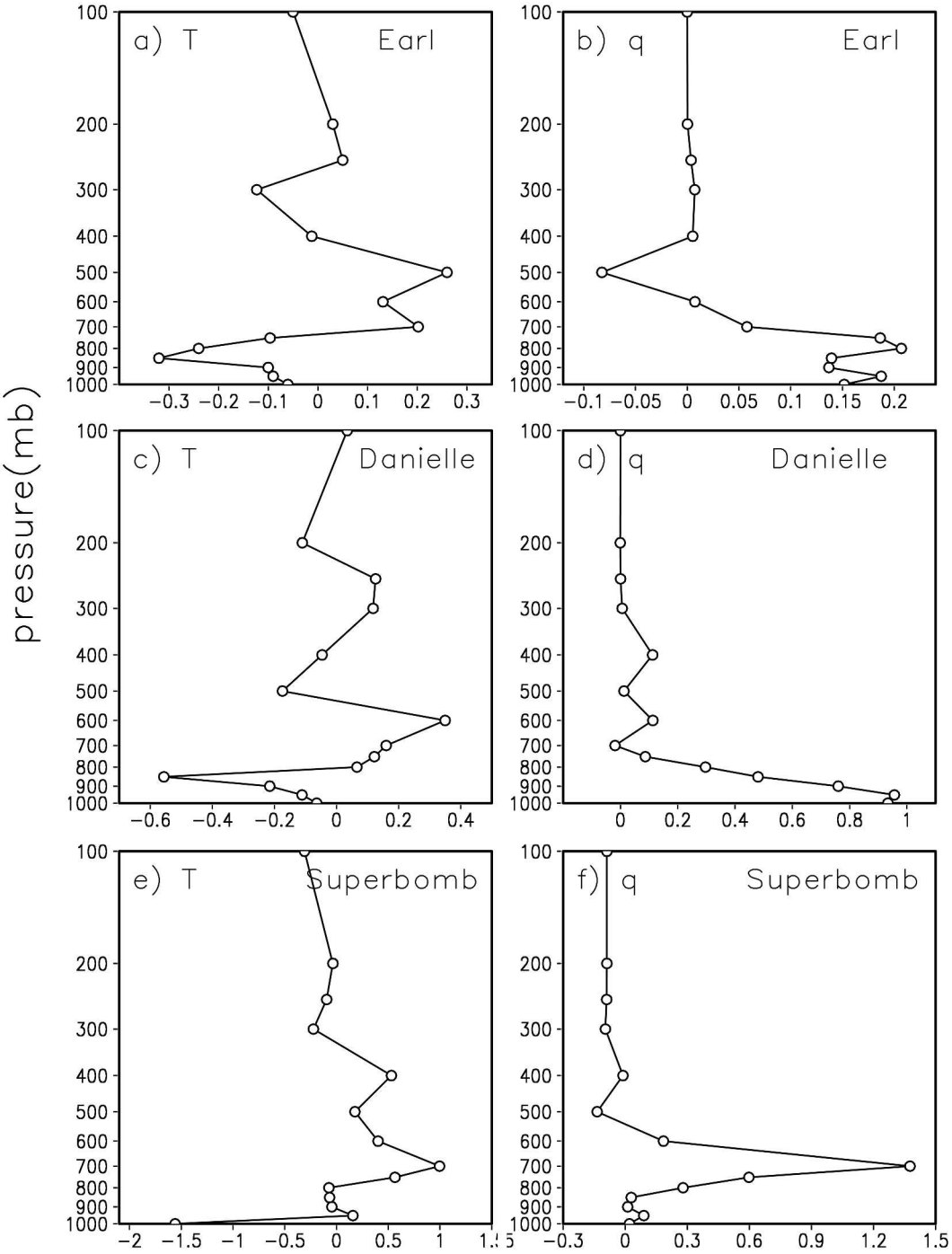

FIG. 10. Vertical profiles of differences in temperature ΔT (°C) and specific humidity Δq (1.0×10^{-3} kg kg^{-1}) at the storm center for simulations with spray *minus* simulations without spray for (a), (b) Earl at (46.3°N, 55.2°W) at 1800 UTC 5 Sep; (c), (d) Danielle at (48.3°N, 18.7°W) at 0000 UTC 6 Sep; and (e), (f) Superbomb at (38°N, 68.5°W) at 0600 UTC 21 Jan. Profiles are area averages over 300^2 km^2 centered at the minimum SLP.

petition with specific humidity differences Δq, which also follow the slanting structure of θ_e (Fig. 11). Figure 12 demonstrates this interplay by showing the contours for ΔT and Δq for Superbomb. As expected, at the storm center, spray enhances the moisture flux from the ocean and cools the boundary layer. However, were it not for the large impact of spray on specific humidity (Figs. 10f, 12b) and implicitly on the mixing ratio, nega-

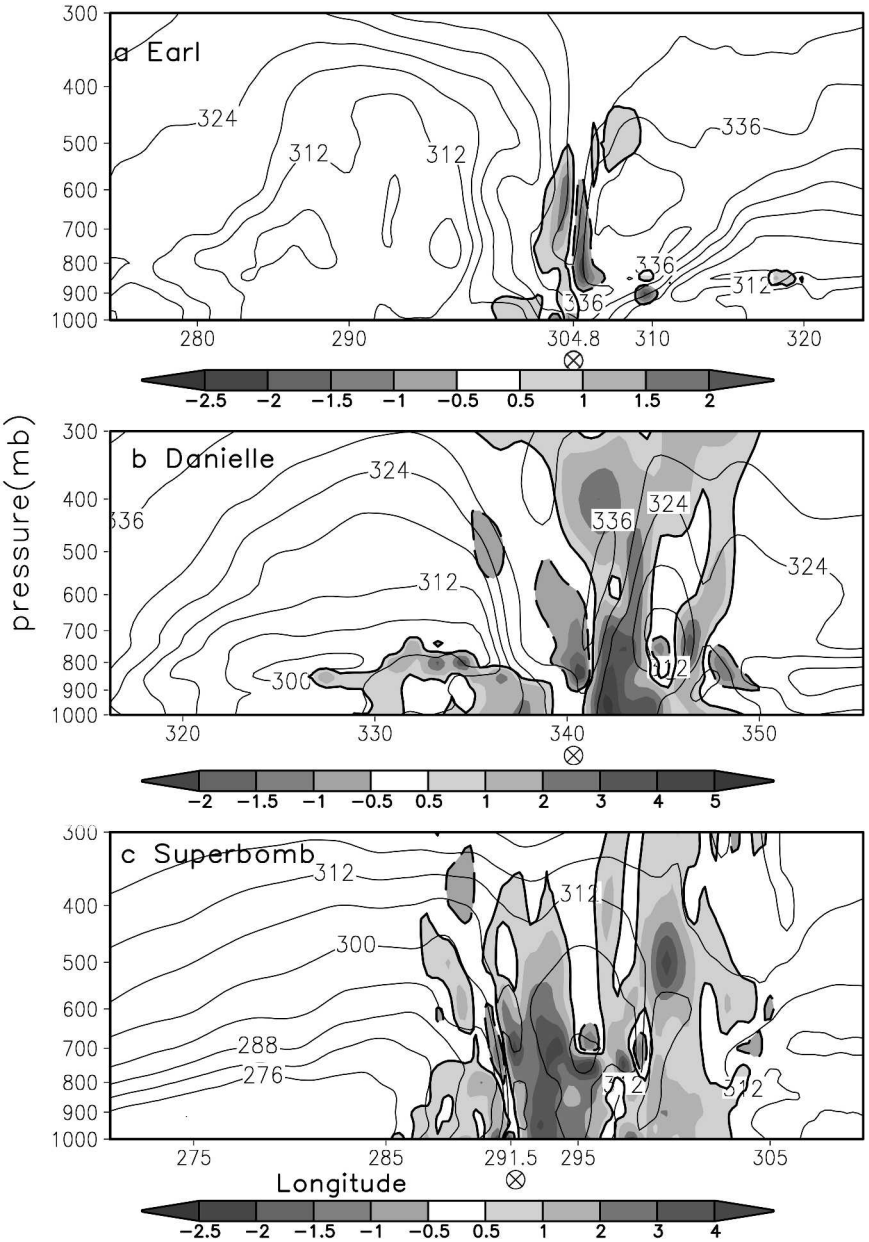

FIG. 11. As in Fig. 10, vertical cross sections, at the time of maximum wind speeds, for equivalent potential temperature, θ_e (contours *without* shading), as a function of longitude through the storm center for (a) Earl at 1800 UTC 5 Sep, (b) Danielle at 1800 UTC 5 Sep, and (c) Superbomb at 0600 UTC 21 Jan. Differences, $\Delta\theta_e$, are shaded contour areas for simulations with spray *minus* simulations without spray at the latent heat flux peaks (Fig. 6). Storm center centers are at 304.8°, 340°, and 291.5°, respectively, as indicated by ⊗. Units are in K.

tive $\Delta\theta_e$ contours would extend to the sea surface. Thus, spray relegates the negative $\Delta\theta_e$ contours to the region from the boundary layer to the midtroposphere at the storm center. The negative $\Delta\theta_e$ contours, in conjunction with the positive $\Delta\theta_e$ contours over the entire storm region, represent the overall spray impact on the cyclone's atmospheric structure.

Why do simulations that include sea spray result in enhanced wind speeds both at the surface and, particularly, at about 800 mb? Spray enhances latent and sensible heat fluxes from the ocean surface to the atmosphere. These fluxes add energy to the storm and thereby produce a lower central pressure and correspondingly higher surface winds (see Fig. 9). The peak enhancement to winds occurs at about 800 mb. This is the level at which the boundary layer winds tend to be

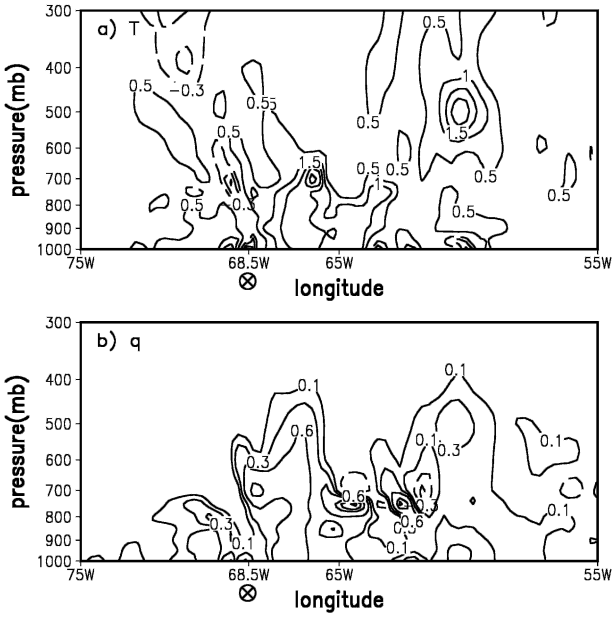

FIG. 12. For Superbomb, the vertical cross sections as a function of longitude for differences between simulations with spray *minus* simulations without spray at the latent heat flux peak (0600 UTC 21 Jan) for (a) temperature (ΔT) and (b) specific humidity (Δq) (1.0×10^{-3} kg kg^{-1}). Storm center (simulation without spray) is at crossed circle ⊗.

highest and also coincides with the largest impacts of sea spray on the vertical profiles of temperature and specific humidity (Figs. 10 and 12). At the 800-mb level, the influence of sea spray on convection is especially strong; thus, the response of the wind field is significant.

5. Conclusions

We investigated the impact of sea spray on numerical simulations of extratropical Atlantic cyclones using a coupled atmosphere and sea spray model. Our analyis focused on two extratropical ex-hurricanes, Earl and Danielle from 1998, and an intense winter storm, Superbomb (2000). We found that including sea spray causes enhanced storm intensity, where U_{10}, area averaged (200^2 km^2) about the peak wind region, is our intensity metric. With spray included in the simulation, U_{10} increases by about 4.8 kt for Earl (10.9%), 7.3 kt for Danielle (13.3%), and 10 kt for Superbomb (14.3%). Spray impacts in the marine boundary layer diminish with increasing height. In terms of area-averaged boundary layer winds, the maximum spray impact tends to occur at about 800 mb and is 4 kt for Earl, 8 kt for Danielle, and 12 kt for Superbomb. These changes in winds reflect spray's direct influence on temperature and humidity in the lower atmosphere that result from increases in the total latent and sensible heat fluxes in the modeled storms. For example, spray enhancements to latent heat fluxes were up to 25 W m^{-2} for Earl, 230 W m^{-2} for Danielle, and 375 W m^{-2} for Superbomb, area averaged (300^2 km^2) around the center of each storm.

As a result of spray in the model simulations, the surface and low-level temperatures are reduced by droplet evaporation, and warming occurs at higher levels, about 500–700 mb. The latter represents a dynamical response to the strong latent heat release associated with recondensing spray-derived vapor around 800 mb (Fig. 10). For simulations of Earl, which show a weak spray impact, the low-level cooling and higher-level warming are about −0.3° and +0.3°C. For Danielle, which experienced a stronger spray impact, low-level cooling and upper-level warming were −0.6° and +0.4°C. Finally, for Superbomb, the most intense of the three storms, low-level cooling and higher-level warming effects were −1.5° and +1.0°C. The combined effect of spray on humidity and temperature can be represented in terms of equivalent potential temperature θ_e, which again shows maximum spray effects near 800 mb near the storm center. Impacts on θ_e are strongest for Superbomb, moderate for Danielle, and much weaker for Earl.

The impacts of spray depend on storm structure and development. Based on the three storms we considered, the factors that most affect how spray influences the surface fluxes and storm development are wind speed, SST, storm propagation speed, and horizontal storm distribution and extent. While our three storms are of comparable spatial extent and degree of asymmetry (Figs. 5a1, 5b1, 5c1), they differ in the other factors mentioned here. For example, Earl propagated rapidly over the warm SST waters and then decelerated markedly over cold waters around Newfoundland (Fig. 2a). It had lower wind speeds than the other two storms; and consequently, the impacts of spray on model simulations are relatively weak. By comparison, Danielle propagated rather slowly over warm SSTs (Fig. 2b) and had higher wind speeds than Earl. The resultant impacts of spray are moderately strong in model simulations. Similarly, Superbomb propagated slowly over warm Gulf Stream SSTs (Fig. 2c) and had very high wind speeds; consequently, the spray impacts are quite strong.

Including a spray parameterization tends to increase overall estimates of storm maximum intensity in comparison with NHC and CMC analyses, and improve wind estimates in comparison with QuikSCAT–NCEP blended winds. However, further conclusive evidence is needed to assess the impact of sea spray on overall simulation skill. Our simulations have considered only the impacts of spray. Related ongoing studies consider the ocean response to the cyclone, including changes to SSTs due to upwelling and related processes, and modifications to sea surface drag due to wind-generated waves, wave breaking, and wave impacts on surface currents.

Acknowledgments. Will Perrie was funded by the (Canada) Panel on Energy Research and Development (Offshore Environmental Factors). Ed Andreas was supported by the U.S. National Science Foundation (Award ATM-00-01037) and the U.S. Office of Naval Research (ONR) (Awards N0001403MP20010 and N0001404MP20091). The Canada Foundation for Climate and Atmospheric Studies (CFCAS) funded J. Gyakum. CFCAS and the Natural Science and Engineering Research Council (NSERC). Funding to the Canada–SOLAS network, as well as ONR funding to GoMOOS (Gulf of Marine Ocean Observing System), provided support for W. Zhang.

REFERENCES

Andreas, E. L, 1990: Time constants for the evolution of sea spray droplets. *Tellus,* **42B,** 481–497.

——, 1992: Sea spray and the turbulent air-sea heat fluxes. *J. Geophys. Res.,* **97,** 11 429–11 441.

——, 1998: A new sea spray generation function for wind speeds up to 32 m s^{-1}. *J. Phys. Oceanogr.,* **28,** 2175–2184.

——, 2002: A review of the sea spray generation function for the open ocean. *Atmosphere–Ocean Interactions*, W. Perrie, Ed., Vol. 1, WIT Press, 1–46.

——, 2003: An algorithm to predict the turbulent air–sea fluxes in high-wind, spray conditions. Preprints, *12th Conf. on Interaction of the Sea and Atmosphere*, Long Beach, CA, Amer. Meteor. Soc., CD-ROM, 3.4.

——, and J. DeCosmo, 1999: Sea spray production and influence on air–sea heat and moisture fluxes over the open ocean. *Air–Sea Exchange: Physics, Chemistry and Dynamics*, G. L. Geernaert, Ed., Kluwer, 327–362.

——, and K. A. Emanuel, 2001: Effects of sea spray on tropical cyclone intensity. *J. Atmos. Sci.,* **58,** 3741–3751.

——, and J. DeCosmo, 2002: The signature of sea spray in the HEXOS turbulent heat flux data. *Bound.-Layer Meteor.,* **103,** 303–333.

——, J. B. Edson, E. C. Monahan, M. P. Rouault, and S. D. Smith, 1995: The spray contribution to net evaporation from the sea: A review of recent progress. *Bound.-Layer Meteor.,* **72,** 3–52.

Bao, J.-W., J. M. Wilczak, J.-K. Choi, and L. H. Kantha, 2000: Numerical simulations of air–sea interaction under high wind conditions using a coupled model: A study of hurricane development. *Mon. Wea. Rev.,* **128,** 2190–2210.

Benoit, R., J. Coté, and J. Mailhot, 1989: Inclusion of a TKE boundary layer parameterization in the Canadian regional finite-element model. *Mon. Wea. Rev.,* **117,** 1726–1750.

——, M. Desgagne, P. Pellerin, Y. Chartier, and S. Desjardins, 1997: The Canadian MC2: A semi-implicit semi-Lagrangian wide-band atmospheric model suited for fine-scale process studies and simulation. *Mon. Wea. Rev.,* **125,** 2382–2415.

Bortkovskii, R. S., 1973: On the mechanism of interaction between the ocean and the atmosphere during a storm. *Fluid Mech.-Sov. Res.,* **2,** 87–94.

Chouinard, C., J. Mailhot, and A. Mitchell, 1994: The Canadian regional data assimilation system: Operational and research applications. *Mon. Wea. Rev.,* **122,** 1306–1325.

DeCosmo, J., 1991: Air–sea exchange of momentum, heat and water vapor over whitecap sea states. Ph.D. dissertation, University of Washington, 212 pp. [Available from UMI Dissertation Services, P.O. Box 1346, Ann Arbor, MI 48106–1346.]

——, K. B. Katsaros, S. D. Smith, R. J. Anderson, W. A. Oost, K. Bumke, and H. Chadwick, 1996: Air-sea exchange of water vapor and sensible heat: The Humidity Exchange over the Sea (HEXOS) results. *J. Geophys. Res.,* **101,** 12 001–12 016.

Emanuel, K. A., 1995: Sensitivity of tropical cyclones to surface exchange coefficients and a revised steady-state model incorporating eye dynamics. *J. Atmos. Sci.,* **52,** 3969–3976.

Fairall, C. W., J. D. Kepert, and G. J. Holland, 1994: The effect of sea spray on the surface energy transports over the ocean. *Global Atmos. Ocean Syst.,* **2,** 121–142.

——, E. F. Bradley, D. P. Rogers, J. B. Edson, and G. S. Young, 1996: Bulk parameterization of air-sea fluxes for Tropical Ocean-Global Atmosphere Coupled-Ocean Atmosphere Response Experiment. *J. Geophys. Res.,* **101,** 3747–3764.

Glickman, T. S., Ed., 2000: *Glossary of Meteorology*. 2d ed. Amer. Meteor. Soc., 855 pp.

Johnson, H. K., J. Højstrup, H. J. Vested, and S. E. Larsen, 1998: On the dependence of sea surface roughness on wind waves. *J. Phys. Oceanogr.,* **28,** 1702–1716.

Kain, J. S., and J. M. Fritsch, 1990: A one-dimensional entraining/detraining plume model and its application in convective parameterization. *J. Atmos. Sci.,* **47,** 2784–2802.

——, and ——, 1993: Convective parameterization for mesoscale models: The Kain–Fritsch scheme. *The Representation of Cumulus Convection in Numerical Models*, *Meteor. Monogr.,* No. 27, Amer. Meteor. Soc., 165–170.

Katsaros, K. B., S. D. Smith, and W. A. Oost, 1987: HEXOS—Humidity Exchange over the Sea, a program for research on water-vapor and droplet fluxes from sea to air at moderate to high wind speeds. *Bull. Amer. Meteor. Soc.,* **68,** 466–476.

Kepert, J. D., C. W. Fairall, and J.-W. Bao, 1999: Modelling the interaction between the atmospheric boundary layer and evaporating sea spray droplets. *Air–Sea Exchange: Physics, Chemistry and Dynamics*, G. L. Greernaert, Ed., Kluwer, 363–409.

Kong, F. Y., and M. K. Yau, 1997: An explicit approach to microphysics in MC2. *Atmos.–Ocean,* **35,** 257–291.

Kuo, Y.-H., R. J. Reed, and S. Low-Nam, 1991: Effects of surface energy fluxes during the early development and rapid intensification stages of seven explosive cyclones in the western Atlantic. *Mon. Wea. Rev.,* **119,** 457–476.

Large, W. G., and S. Pond, 1981: Open ocean momentum flux measurements in moderate to strong winds. *J. Phys. Oceanogr.,* **11,** 324–336.

Li, W., W. Perrie, E. L Andreas, J. Gyakum, and R. McTaggart-Cowan, 2003: Impact of sea spray on numerical simulation of extratropical hurricanes. Preprints, *12th Conf. on Interaction of the Sea and Atmosphere*, Long Beach, CA, Amer. Meteor. Soc., CD-ROM, 2.5.

Liu, W. T., K. B. Katsaros, and J. A. Businger, 1979: Bulk parameterization of air-sea exchanges of heat and water vapor including the molecular constraints at the interface. *J. Atmos. Sci.,* **36,** 1722–1735.

Ling, S. C., and T. W. Kao, 1976: Parameterization of the moisture and heat transfer process over the ocean under whitecap sea states. *J. Phys. Oceanogr.,* **6,** 306–315.

McTaggart-Cowan, R., 2003: A potential vorticity component-based study of the extratropical transitions of hurricanes Danielle and Earl (1998). Ph.D. thesis, McGill University, 224 pp.

——, J. R. Gyakum, and M. K. Yau, 2001: Sensitivity testing of extratropical transitions using potential vorticity inversions to modify initial conditions: Hurricane Earl case study. *Mon. Wea. Rev.,* **129,** 1617–1636.

——, ——, and ——, 2004: The impact of tropical remnants on extratropical cyclogenesis: Case study of Hurricanes Danielle and Earl (1998). *Mon. Wea. Rev.,* **132,** 1933–1951.

Meirink, J. F., and V. K. Makin, 2001: Impact of sea spray evaporation in a numerical weather prediction model. *J. Atmos. Sci.,* **58,** 3626–3638.

Riehl, H., 1954: *Tropical Meteorology*. McGraw-Hill, 392 pp.

Robert, A., T. Yee, and H. Ritchie, 1985: A semi-Lagrangian and semi-implicit numerical integration scheme for multilevel atmospheric models. *Mon. Wea. Rev.,* **113,** 388–394.

Rouault, M. P., P. G. Mestayer, and R. Schiestel, 1991: A model

of evaporating spray droplet dispersion. *J. Geophys. Res.,* **96,** 7181–7200.

Sanders, F., and J. R. Gyakum, 1980: Synoptic–dynamic climatology of the "bomb." *Mon. Wea. Rev.,* **108,** 1589–1606.

Smith, S. D., 1988: Coefficients for sea surface wind stress, heat flux, and wind profiles as a function of wind speed and temperature. *J. Geophys. Res.,* **93,** 15 467–15 472.

——, K. B. Katsaros, W. A. Oost, and P. G. Mestayer, 1990: Two major experiments in the Humidity Exchange over the Sea (HEXOS) program. *Bull. Amer. Meteor. Soc.,* **71,** 161–172.

——, and Coauthors, 1992: Sea surface wind stress and drag coefficients: The HEXOS results. *Bound.-Layer Meteor.,* **60,** 109–142.

Thorncroft, C. D., B. J. Hoskins, and M. E. McIntyre, 1993: Two paradigms of baroclinic-wave life-cycle behaviour. *Quart. J. Roy. Meteor. Soc.,* **119,** 17–55.

Wang, Y., J. D. Kepert, and G. J. Holland, 2001: The impact of sea spray evaporation on tropical cyclone boundary layer structure and intensity. *Mon. Wea. Rev.,* **129,** 2481–2500.

Wu, J., 1973: Spray in the atmospheric surface layer: Laboratory study. *J. Geophys. Res.,* **78,** 511–519.

——, 1974: Evaporation due to spray. *J. Geophys. Res.,* **79,** 4107–4109.

——, 1982: Wind-stress coefficients over sea surface from breeze to hurricane. *J. Geophys. Res.,* **87,** 9704–9706.